Invited Paper

Angular dependence of sampling MTF

O. Hadar,[1] A. Dogariu,[2] and G. D. Boreman[2]
1. Ben-Gurion University of the Negev
Department of Electrical and Computer Engineering
P.O.Box 653
84105 Beer-Sheva, ISRAEL
2. University of Central Florida
Center for Research and Education in Optics and Lasers
Orlando, FL 32816-2700

Abstract

Sampling MTF defined in Park,[1] Hock,[2] and de Luca,[3] as an x and y sampling, can be generalized for image data not along x and y directions. For a given sampling lattice (such as in a laser printer, a scene projector, or a focal plane array), we construct a two-dimensional sampling MTF based on the distance between nearest samples in each direction. Because the intersample distance depends on direction, the sampling MTF will be best in the directions of highest spatial sampling, and poorer in the directions of sparse sampling. We compare hexagonal and rectangular lattices in terms of their equivalent spatial frequency bandwidth. We filter images as demonstration of the angular-dependent two-dimensional sampling MTF.

Keywords : Two-dimensional MTF, image-sampling, image processing .

1. Introduction

In this paper, the effect of two-dimensional sampling on image quality is investigated with two different lattice structures. A finite-sized sampling lattice yields discrete image-sampling directions and a sample-to-sample distance that varies with direction. Angles with close nearest neighbors will have high resolution while other angles will produce poorer resolution. The number of angles and the distance between samples will determine the image quality resulting from the sampling process. As we increase the number of lattice points, the number of possible discrete angles will increase and the total resolution will increase. In the first section the mathematical development for average sampling MTF in one dimension is derived. Next we describe the derivation as a nonseparable two-dimensional sampling MTF from the definition of the one-dimensional average sampling MTF. The process of obtaining the MTF is then demonstrated on two different lattices, rectangular and hexagonal. An equivalent bandwidth for the MTF is defined in the next section on the basis of noise-equivalent bandwidth. This figure of merit is used for comparison of different lattice sizes and configurations. We then present a simulator of these results on a test image.

2. Average Sampling MTF

Previous work in sampling MTF [1-3] has been performed only in the context of x- and y-domain sampling. Here we consider both the two orthogonal directions and all other possible directions. Any sampling grid has different spatial sampling rates in different directions. This paper presents the sampling MTF as a two-dimensional sampling system. This analysis has applications to laser-printers systems, infrared scene projectors, and focal-plane arrays.

In the case of one-dimensional sampling MTF, two MTF functions are involved in the sampling process[2]: the MTF as result of the pixel size, MTF_{pixel}, and the MTF caused by the spatial sampling rate, MTF_{samp}.

For a rectangular pixel, the pixel MTF is given by the well-known sinc-function formula

$$MTF_{pixel} = \mathrm{sinc}(\xi\, p) \qquad (1)$$

where $\mathrm{sinc}(x) = (\sin \pi x)/(\pi x)$, ξ is the image spatial frequency, and p is the pixel size. The square pixel is the most common shape for imaging-array applications, although other shapes are possible such as circular, hexagonal,[4] or tapered.[5]

SPIE Vol. 3110 • 0277-786X/97/$10.00

The MTF in Eq. (1) does not account for the distance between the samples. We derive the sampling MTF from the pixel MTF [Eq. (1)]. The independence of these two processes allows us to multiply these two MTFs to derive the total MTF of the sampling process and spatial average. In this paper we will concentrate on the sampling MTF.

The sampling MTF results from a reduction in measured modulation depth because the image data can exist at a random location with respect to the sampling sites. Park[1] performs an average MTF calculation over all relative positions of the image data with respect to the sampling sites. This statistical approach performs an average of the shift-variant image quality that is seen in sampled data systems, to define a shift-invariant average MTF. The derivation of the one-dimensional sampling MTF is based on statistical treatment of the intensity sampled by the array of pixels.[1-3] The image-quality effect of sampling is equivalent to a convolution of the image data with a rectangular function, whose width is equal to the sampling interval.[1] Thus, the sampling MTF is a *sinc* function, with first zero equal to the inverse of the 1/(sampling interval).

The *sinc* function[1], can be obtained in a simple intuitive manner. Assume a sinusoid, with a spatial period X and unity amplitude. We calculate the expected value of the modulation depth M of this sinusoid as a function of spatial sampling interval Δ and the spatial frequency $\xi = 1/X$. The sampling grid can have statistically any phase φ with respect to the maxima and minima of the sinusoid.

We can begin with the expression for modulation depth,[3]

$$M(\xi,\Delta,\varphi) = (A_{max}-A_{min})/2 \tag{2}$$

Where A_{max} and A_{min} are respectively the maximum and the minimum sampled values. If we define φ as the smallest distance between the sampling grid and the positive crest of the sine waves, measured from this crest, φ varies between $\varphi_{min} = -\Delta/2$ and $\varphi_{max} = \Delta/2$.

Two extreme cases for the value M can be obtained from the sampling process. The maximum value is obtained for $\varphi = 0$, $M_{max} = 1$ while the minimum value, M_{min} is obtained for $\varphi = \varphi_{min} = -\Delta/2$ or $\varphi = \varphi_{max} = \Delta/2$. The value of M_{min} can be found using simple trigonometric identity,

$$M_{min} = 2\cos(2\pi\xi\frac{\Delta}{2})/2 = \cos(\pi\xi\Delta), \tag{3}$$

Between extreme cases MTF_{min} and MTF_{max} are many different MTFs that can be derived from different values of the phase φ between the sine wave and the sampling grid. It is possible to obtain the average MTF by performing averaging over all possible locations of the sampling lattice with respect to the waveform. The assumption is that the random variable φ is equally distributed between $\varphi_{min} = -\Delta/2$ and $\varphi_{max} = \Delta/2$ with a uniform probability density function

$$f_\varphi(\varphi) = \begin{cases} 1/\Delta, & for \ -\Delta/2 \le \varphi \le \Delta/2 \\ 0, & elsw here \end{cases} \tag{4}$$

The average MTF (AMTF) is defined by the integral,

$$AMTF_{samp}(\xi,\Delta) = \int_{-\Delta/2}^{\Delta/2} f_\varphi(\varphi)M(\xi,\Delta,\varphi)d\varphi = \frac{1}{\Delta}\int_{-\Delta/2}^{\Delta/2}\cos(\pi\xi\varphi)d\varphi = \sin c(\xi\Delta), \tag{5}$$

The result of Eq. (5) can be interpreted as follow. For a nonzero sampling interval of Δ, we will not obtain the true maxima and minima of the sinusoid on an average basis, but rather will obtain an average maximum and average minimum value of the sinusoid that are the average values of the waveform over the interval Δ. The maximum average value of the waveform is the average of the peak of the sinusoid

over an interval Δ, while the minimum average value of the waveform is the average of the valley of the sinusoid over the same interval. This conceptual model yields the main result of Park,[1] namely the *sinc* function with the first zero location $\xi_{cutoff} = 1/\Delta$. Even for very sparse sampling, where the spatial sampling interval Δ is less than the Nyquist requirement of 1/2X, the notion of an average maximum value and average minimum value is still valid, even when the averaging is performed over an interval Δ that is greater than half the period of the waveform. Obviously, as Δ increases (sparser sampling) because the difference between maximum and minimum average values will decrease, both averages have already taken averages over more than half of the sinusoid.

The result of Eq. (5) can be modified for the case of two-dimensional sampling by representing the MTF for the two orthogonal axes *x* and *y* ,

$$\mathrm{MTF}(\xi) = \mathrm{Sinc}(\xi\Delta_x) = \frac{\sin(\pi \cdot \xi \cdot \Delta_x)}{(\pi \cdot \xi \cdot \Delta_x)} \tag{6a}$$

$$\mathrm{MTF}(\eta) = \mathrm{Sinc}(\eta\Delta_y) = \frac{\sin(\pi \cdot \eta \cdot \Delta_y)}{(\pi \cdot \eta \cdot \Delta_y)} \tag{6b}$$

where ξ and η are the spatial frequencies in the *x* and *y* axes respectively and Δ_x and Δ_y are the sampling interval in the *x* and *y* axes respectively. We allow the MTF to be a bipolar function rather than using the magnitude.

It should be noted that these equations do not imply a separable two-dimensional MTF as the product of Eqs. (6a) and (6b). The sampling interval and associated sampling MTF for spatial frequencies not along *x* or *y* will be calculated separately.

3. Definition of a nonseparable two-dimensional sampling MTF

In this section the main steps of deriving the sampling MTF for both rectangular and hexagonal lattices are described. We develop the MTF not only along the ξ and η but also along the other directions that are involved in the sampling process. For any given lattice with a finite size and shape, a finite number of directions (angles) carry information after the sampling process. These directions can be derived from all of the possible lines that can be reproduced by the lattice. We assume that each of these lines passes exactly through the center of sampling points in the grid. The main extension of our work from that of previous authors is that we use the *sinc* function of Eq. (5) as valid for any sampling direction in a two-dimensional lattice. This allows us to calculate a sampling MTF in any direction of the lattice.

We show portions of the two sampling lattices (rectangular and hexagonal) investigated in Fig. 1(a) and (b). We define the distance between two adjacent points of the rectangular lattice in the *x* and *y* directions as Δ. If we take the lower left point of the grid as the origin of the lattice, then any other point in the lattice has a certain distance from origin point Δ_θ , which is a function of Δ and θ , the angle between the point and the positive direction of the *x* axis. For example, the sampling distance for the five highest-resolution directions in the lattice in a sector of 90^o are $\Delta_{0^\circ} = \Delta_{90^\circ} = \Delta$, $\Delta_{45^\circ} = \sqrt{2} \cdot \Delta$, and $\Delta_{26.56^\circ} = \Delta_{63.44^\circ} = \sqrt{5} \cdot \Delta$. For other angles, the sampling is less frequent, and the *sinc* function associated with the sample-to-sample distance will have a correspondingly lower cutoff frequency. The *sinc* function MTF of Eq. (5) can be generalized to a nonseparable equation in terms of a two-dimensional spatial frequency ξ_θ where the wavevector for any particular spatial frequency is along the θ direction,

$$\mathrm{MTF}(\xi_\theta) = \mathrm{sinc}(\xi_\theta \Delta_\theta) = \sin(\pi\xi_\theta \Delta_\theta) / (\pi\xi_\theta \Delta_\theta). \tag{7}$$

In Fig. 1(b) the same analysis is implemented for the hexagonal lattice. Let us set the sampling distance along the x direction $\Delta_0 = \Delta$ to be equal for both the square lattice and the hexagonal lattice. We construct the hexagonal lattice from the rectangular lattice by moving the odd rows a distance of $\Delta/2$ to the right, and setting the distance between rows in the vertical direction to $\frac{\sqrt{3}}{2}\Delta$. This configuration provides us a symmetric lattice within a 60° sector. This kind of lattice is particularly appropriate for printing applications because it is the most compact lattice[6] for round pixels.

For the hexagonal lattice of Fig. 1(b), the minimum sample distance is $\Delta_0 = \Delta_{60}$. The highest-resolution directions in the 60° sector with their sampling distances are $\Delta_{0^\circ} = \Delta_{60^\circ} = \Delta$, $\Delta_{30^\circ} = \sqrt{3}\cdot\Delta$, and $\Delta_{19.1^\circ} = \Delta_{49.1^\circ} = \sqrt{7}\cdot\Delta$. The MTF here is also a function of the sampling direction as in Eq. (7).

The application of Eq. (7) will yield a nonseparable MTF with *sinc* functions in each direction. This function is difficult to visualize because of its discontinuous variation with angle.

Figures 2(a) and (b) represent the three highest-resolution MTFs in the rectangular lattice and the hexagonal lattice plotted as function of $|\xi_0|$ respectively.

We can obtain a more complete picture of the angular dependence of the MTF by using a top view. In Fig. 3 we plot a line in each direction, whose length in that direction is equal to the distance along ξ_θ to the first zero of the *sinc* function in that direction. Figures 3(a) and (b) show the results in a 90° sector for a 10-by-10 lattice size for both rectangular lattice and hexagonal lattice respectively. A long line in a certain direction represents high resolution in that direction. For each lattice, the MTF is a discontinuous function of angle θ, with some directions having high resolution, some with low resolution, and some directions having MTF = 0 (no sampling in that direction).

4. An equivalent-bandwidth figure of merit

In this section a useful measure for quantifying the sampling process will be defined. The equivalent bandwidth of the *sinc* function for any direction in the lattice will be derived. A common definition for equivalent bandwidth is the equivalent-noise bandwidth.[7] We thus define angle-dependent bandwidth :

$$BW_\theta = \frac{1}{MTF_\theta(0)}\int_0^\infty MTF_\theta(\xi)d\xi, \tag{8}$$

where $MTF_\theta(\xi)$ is the MTF in a certain angle θ relative to the x direction, and $MTF_\theta(0)$ is the maximum value of the MTF, which is unity. To compare the image-quality performance for various lattice sizes and configurations, we use the equivalent bandwidth (BW) of the *sinc* function as the MTF in Eq. (8),

$$BW_\theta = \int_0^\infty \mathrm{sinc}(\xi_\theta \Delta_\theta)d\xi = \frac{1}{\Delta_\theta}. \tag{9}$$

Equation (9) has the simple geometric interpretation as the distance to first zero ($1/\Delta_\theta$), which defines the ξ_{cutoff} of the *sinc* function, shown as the length of the line in the plot in Fig. (3).

We can write BW_θ in each possible direction of the lattice as function of Δ, which is the basic sampling interval along the x axis ($\Delta_{0^\circ} = \Delta$),

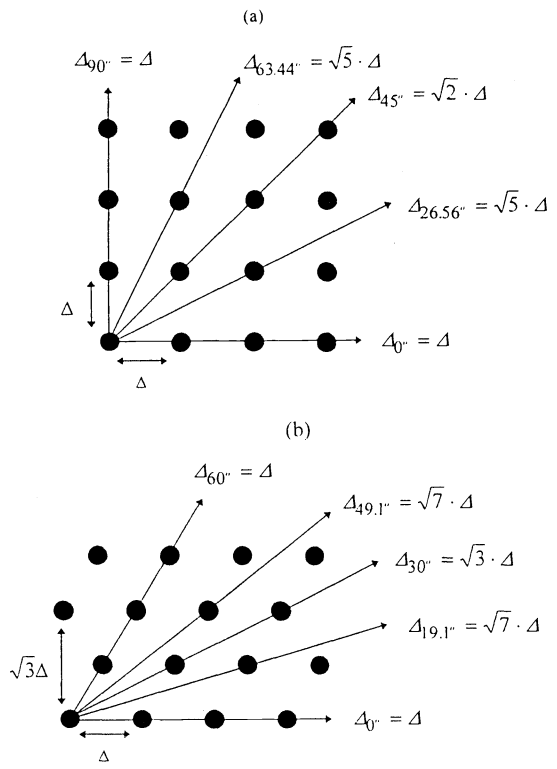

Fig. 1 A 4 by 4 lattice size with the high resolution directions marked by arrows , (a) Rectangular lattice (b) Hexagonal lattice

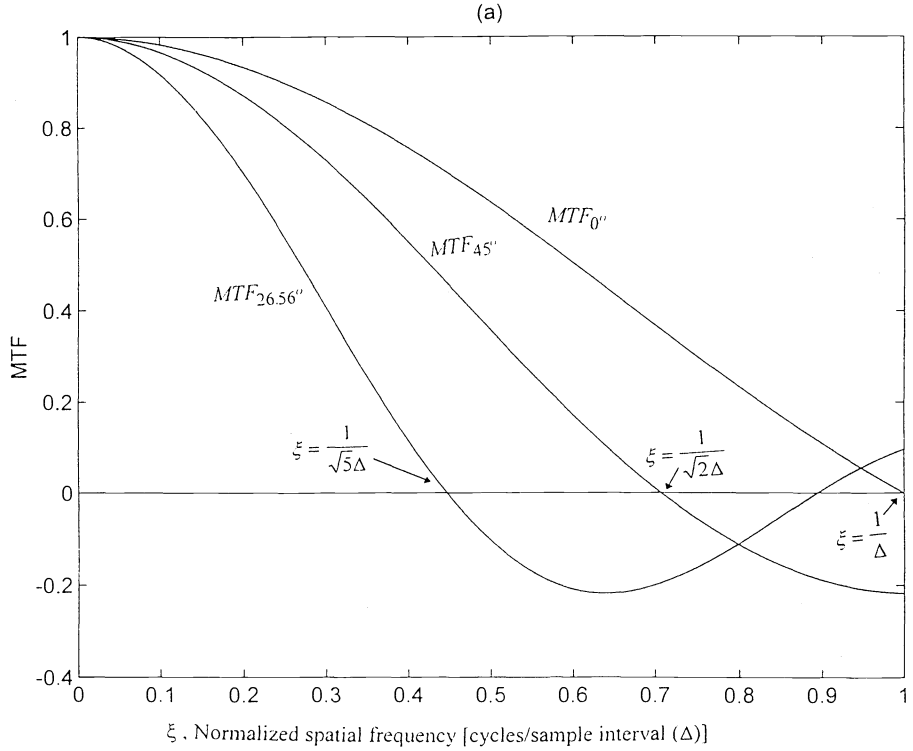

Fig.2 The three highest resolution MTFs in a 1D plot, (a) Rectangular lattice (b) Hexagonal lattice.

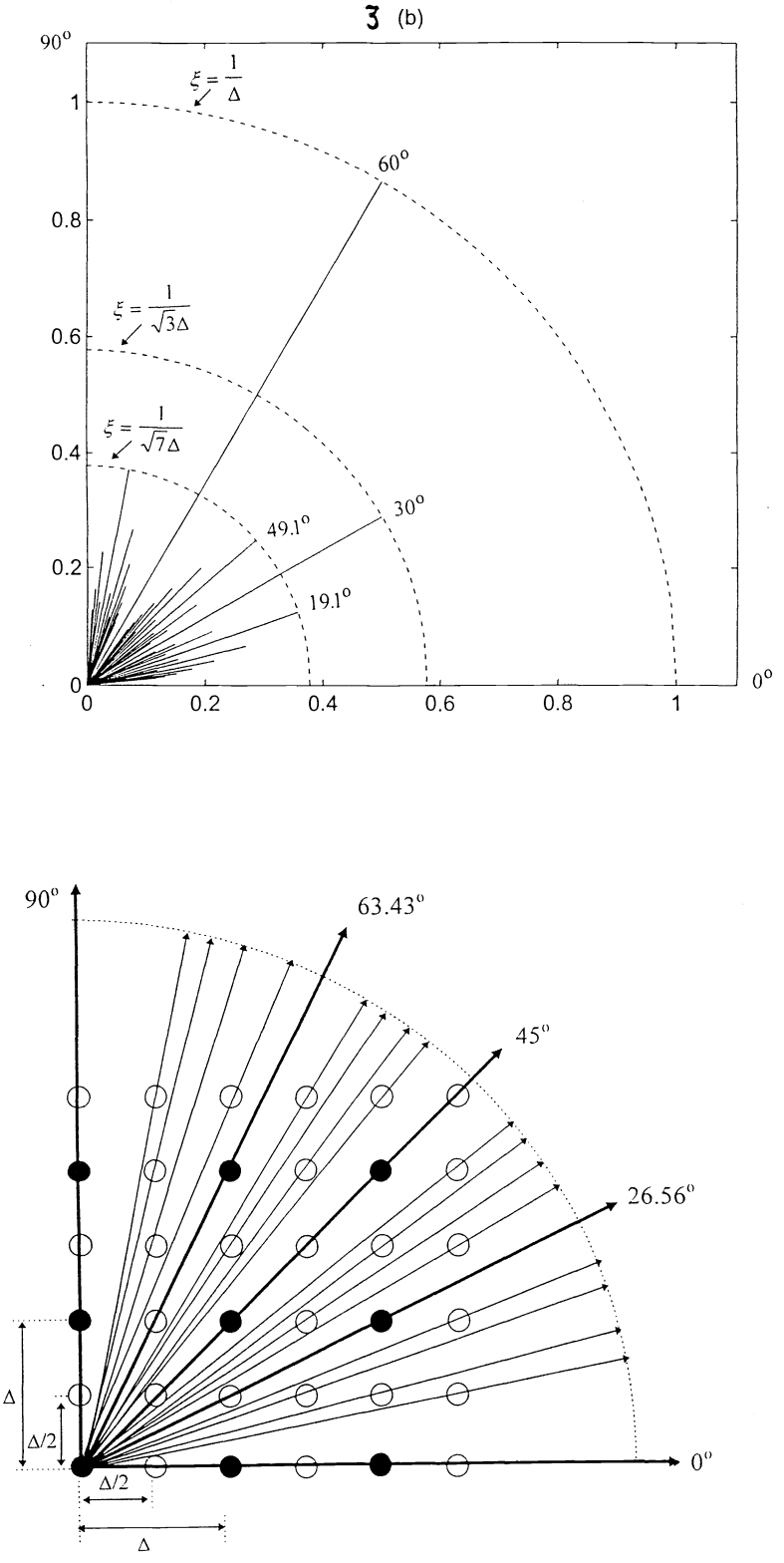

Fig. 4. Scaling the cutoff frequency for doubling the lattice size, original 3 by 3 points rectangular lattice (closed circles), 6 by 6 points rectangular lattice (open circles).

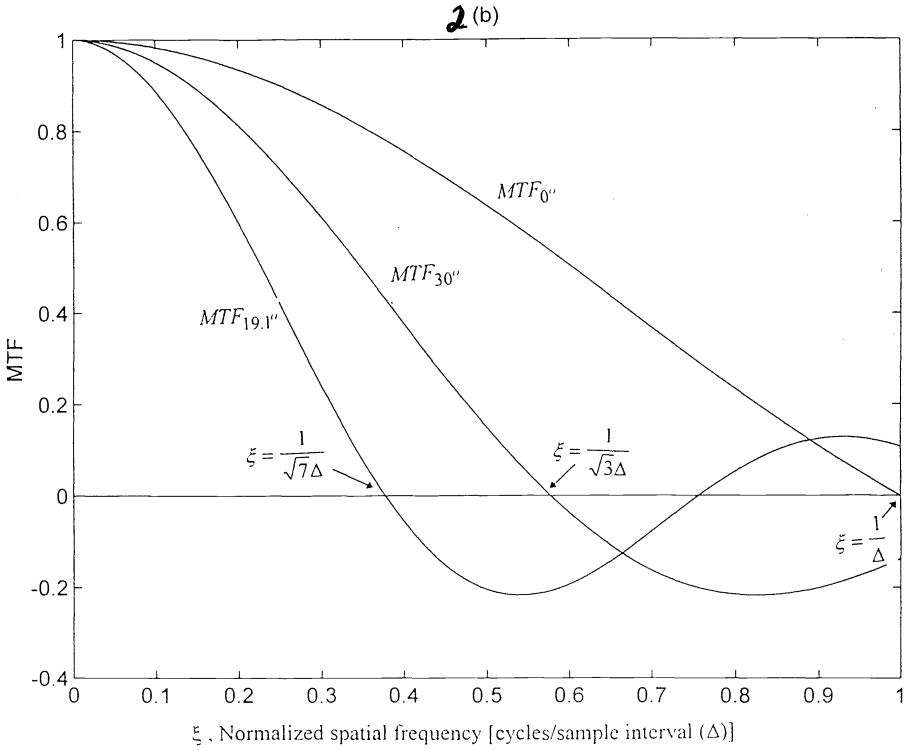

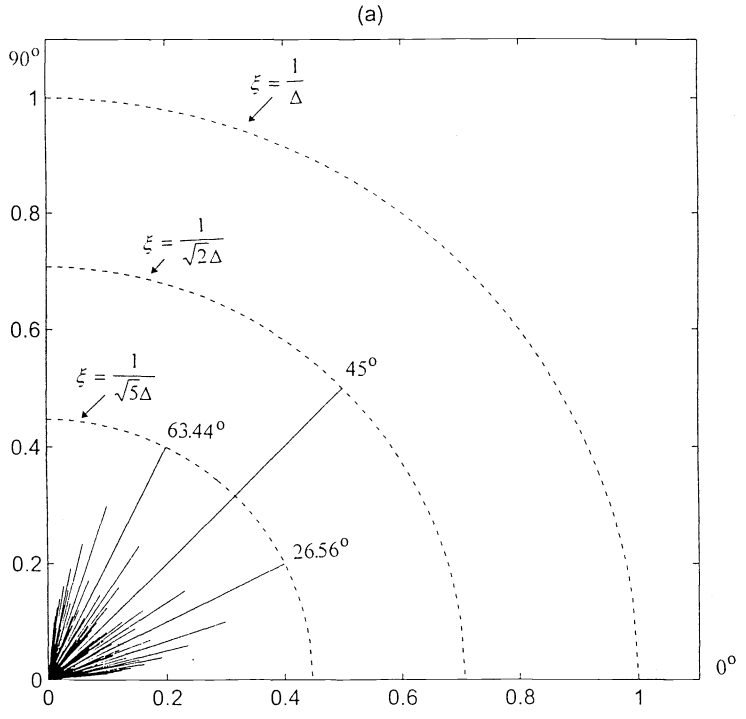

Fig. 3 The first zero location of the MTF as function of the angle θ in a radial plot : (a) Rectangular lattice (b) Hexagonal lattice.

$$BW_\theta = \frac{1}{\Delta_\theta} = k_\theta \cdot \frac{1}{\Delta} \tag{10}$$

where k_θ is a constant representing the length of a certain line in Fig. (3) in units of $1/\Delta$.
To construct a figure of merit for any given lattice, we sum up the BWs for all of the possible directions. This will give a total BW, BW_{total}, for the sampling lattice, and can be interpreted as the area in polar coordinates under the curves plotted in Fig. (3),

$$BW_{total} = \sum_{\theta=0^\circ}^{\theta=90^\circ} BW_\theta = \sum_{\theta=0^\circ}^{\theta=90^\circ} k_\theta \cdot \frac{1}{\Delta} = K \cdot \frac{1}{\Delta} \tag{11}$$

where K is the sum of all the k_θ constants that exist between $\theta = 0^\circ$ and $\theta = 90^\circ$.

The new measure BW_{total} allows us to investigate the influence of increasing the lattice size on the image quality. The difference in image quality in using a larger lattice is twofold: one increase is from the larger number of angles for which there exists a nearest neighbor. This will tend to "fill in" the angles for which the MTF is small but not exactly equal to zero. The second and most important reason for an increase in image quality in using a larger lattice is that for a given image field size, more sampling points imply a higher spatial sampling rate, with higher cutoff frequencies in all directions.

In Fig. 4 the influence of doubling the lattice size on the total frequency bandwidth of the sampling system is demonstrated. The original rectangular lattice has a size of 3-by-3 points (close circles) with sampling interval of Δ in the two main orthogonal axis x and y. The number of angles for this case is 5 and they are marked by the thick arrows at 0°, 26.56°, 45°, 63.44°, and 90°. The higher-resolution lattice shown as the 6-by-6 array of open circles, contains twice the number of points as the lower-resolution lattice. The sampling rate increases by factor of 2 in these directions and the sampling interval decreases from Δ to $\Delta/2$ in the x and y axes.

The second reason for increasing the resolution is the additional angles in the higher-resolution lattice. More than 20 possible directions (thin short arrows) are seen as four new directions between each two of the former directions. These angles contribute to the summation of BW_θ in the larger lattice

For comparison of different lattice configurations on this basis (square vs hexagonal) we keep the total number of lattice points equal (100 points in a 10-by-10 square, and 100 points in the hexagonal). This allows us to compare directly the BW_{total} as a figure of merit. The results for this comparison are, for the rectangular lattice, BW_{total} = 111.44 [Cy/Δ] and for the hexagonal lattice, BW_{total} = 126.01 [Cy/Δ] . There is a 13% benefit from using the hexagonal lattice compared to the rectangular lattice for a 10- by-10 lattice size.

We investigate the influence of increasing the number of points of the lattice in one-dimension N (lattice size equal to N x N), on the total number of angles.

Figure 5 represents the number of possible angles for both rectangular and hexagonal lattices as function of N. We take the lower left point of the grid and consider it as the reference point for the all other points in the lattice.

For both lattices, increasing the number of points of the lattice produces more possible angles. However the rate of increase of possible angles in the case of the hexagonal lattice is higher than in the case of the rectangular lattice. Analytical functions have been fitted for both the numerical functions in Fig. 5, $0.58N^2$ for the rectangular lattice and $0.63N^2$ for the hexagonal lattice. This means that there are 8.6% of N^2 more angles in the hexagonal lattice than in the rectangular lattice for the same number of sampling points in the lattice.

Influence of N on BW_{total}

Lets discuss now the influence of increasing the number N on the new measure BW_{total}. The basis for this calculation is to keep the lattice size at constant value and change only the number of points in the lattice. By incrementing the number of lattice points, the sampling distance decreases and the spatial

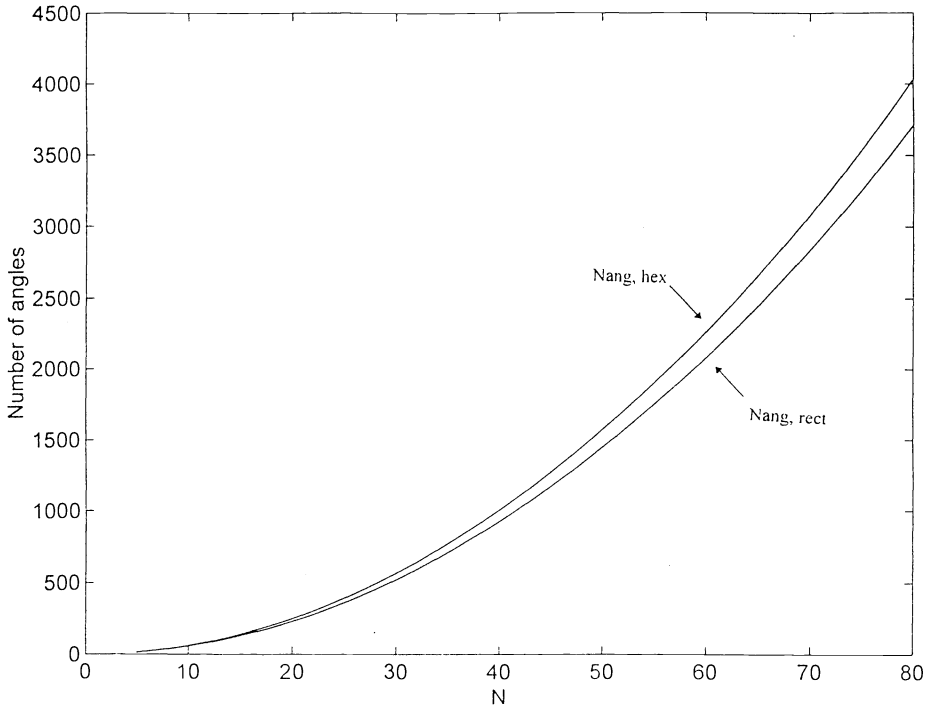

Fig. 5. Number of possible angles as a function of number of points in 1D , N (lattice size equals N by N points).

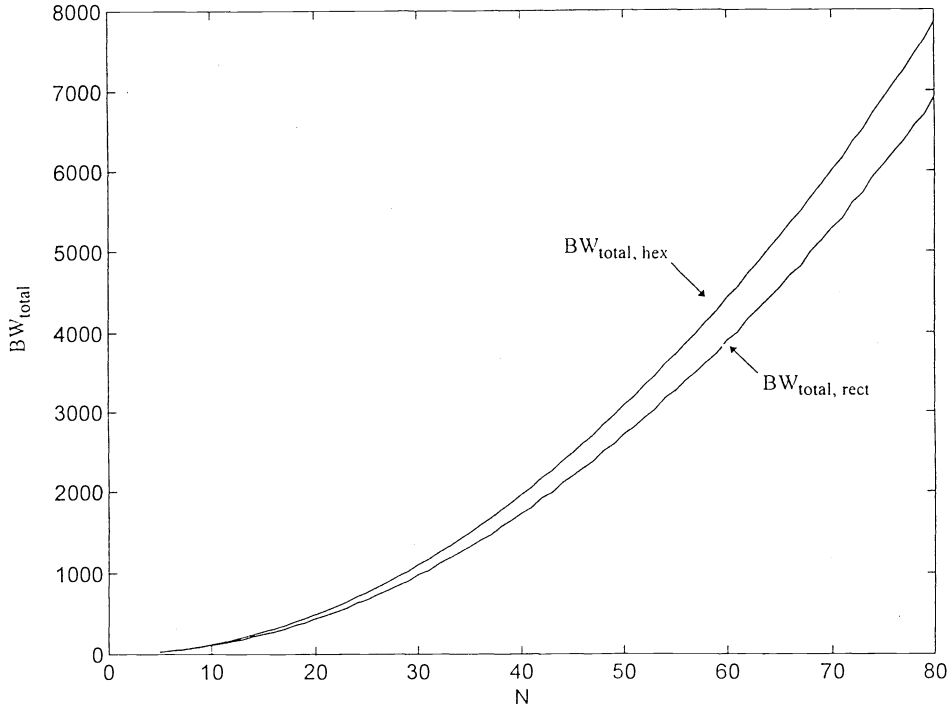

Fig. 6. Total equivalent bandwidth BW_{total} as function of N.

frequency is scaled each time to the new sampling rate. Figure 6 represents the results for BW_{total} for both the rectangular and the hexagonal lattice, where BW_{total} is plotted as function of N. As expected, BW_{total} increases with increasing the value of N for both lattices, because both the sampling rate and the number of possible angles increase. BW_{total} is always higher for the hexagonal lattice. This result was expected because 1) the distance between rows in the hexagonal lattice is smaller by 15.4% when compared to the rectangular lattice; 2) the number of angles in the hexagonal lattice is higher. Analytical functions for the dependence of BW_{total} of N as been fitted to the numerical results. For the rectangular lattice, BW_{total} is $1.09N^2$ and for the hexagonal lattice, BW_{total} is $1.23N^2$. There is a 13% benefit to choosing the hexagonal lattice for any lattice size.

5. Pictorial comparison/demonstration

We constructed the sampling MTF for a given lattice size and configuration. The original image is 512 by 512 pixels. The degradation process is described by the block diagram in Fig. (7). The first step is to derive all the possible directions for which information can be reproduced by the lattice in a sector of 90° (a quarter of the original sampling lattice size). For our purposes, the origin of the lattice is determine to be the center point of the lattice. The next step is to associate a *sinc* function with each of these directions and scale the cutoff of the *sinc* to correspond with the desired cutoff frequency. The MTF is than multiplied by the Fourier transform of the original image. The degradation sampling is associated only with decrease of the amplitude. The MTF is thus applied only on the magnitude of the image Fourier transform. Thus, the original phase is kept while the amplitude is degraded by the MTF. The lines in Fig. 7 indicate the existing directions for a given lattice, where the amplitude is multiplied by the MTF. All the other directions of the original image amplitude are set to zero. Using the degraded amplitude function combined with the original phase function and taking the inverse Fourier transform gives us the degraded image in the spatial domain.

The original image is plotted in Fig. 8; it is a black ring on a white background with a width of 10 pixels and inner radius of 90 pixels. The image is degraded by a sampling MTF corresponding to 100 by 100 lattice size of rectangular lattice and hexagonal lattice are presented in Fig. 9 a and b respectively. The degraded image is unequally degraded in different angles. The blur size is not equal in all the directions of the blurred image. In the image degraded by the rectangular lattice (Fig. 9(a)) the least degraded directions are the x and y directions, indicating that these directions are more prominent than the others. This phenomenon can be shown by the sharp edges of the thin lines in these directions. All the other directions are more degraded and have smeared edges. Also it can be shown that the degraded image is symmetrically degraded within a cycle of 90° sector.

In the image degraded by the hexagonal lattice (Fig. 9b) the x and y direction are also more prominent than the other directions. It can be seen that the two lines perpendicular to the x direction are sharper than the lines that perpendicular to the y direction. The reason is that in the hexagonal lattice the resolution in the x direction is higher than the resolution in the y direction by factor of $\sqrt{3}$.

6. Conclusions

An average MTF for the sampling process has been obtained by an average over the sampling locations sampling of a sine wave. The result MTF is the *sinc* function with the first zero location at the reciprocal of the sampling interval. The *sinc* function MTF has been generalized to a nonseparable MTF in terms of a two-dimensional spatial frequency at all the possible directions of the sampling lattice. The main extension of this work from that of previous authors is that we use the *sinc* function as valid for any sampling direction in a two-dimensional lattice. The MTF derivation has been demonstrated for two lattice configurations, rectangular lattice and hexagonal lattice. A useful quantitative measure as been defined as the total equivalent bandwidth of the sampling lattice. This measure allows us to compare different lattice configuration and size. A pictorial demonstration as been presented for two different lattices.

7. Acknowledgment

This work was supported by the Hewlett-Packard University Grants Program and the Clore scholar Foundation for doctoral students in Israel.

8. References

1. S. K. Park, R. Schowengerdt, and M. A. Kaczynski, "Modulation-transfer-function analysis for sampled image systems," *Appl. Opt.* **23**, 2572-2582 (1984) .
2. K. M. Hock, "Effect of oversampling in pixel arrays," *Opt. Eng.* **34**, 1281-1288 (1995).
3. L. de Luca and G. Cardone, "Modulation transfer function cascade model for a sampled IR imaging system," Appl. Opt. **13**, 1659-1664 (1991) .
4. K. J. Barnard and G. D. Boreman, "Modulation transfer function of hexagonal staring focal plane arrays," *Opt. Eng.* **30**, 1915-1919 (1991).
5. G. Boreman and A. Plogstedt, "Spatial filtering by a line-scanned nonrectangular detector application to SPRITE readout MTF," *Appl. Opt.* 28, 1165-1168 (1989).
6. N. W. Ashcroft, and N. D. Mermin, *Solid State Physics,* pp. 63-83, Saunders College, Philadelphia (1976).
7. R. D. Hudson, Jr., *Infrared System Engineering,* pp. 311-315, John Wiley & Sons, New York (1969).

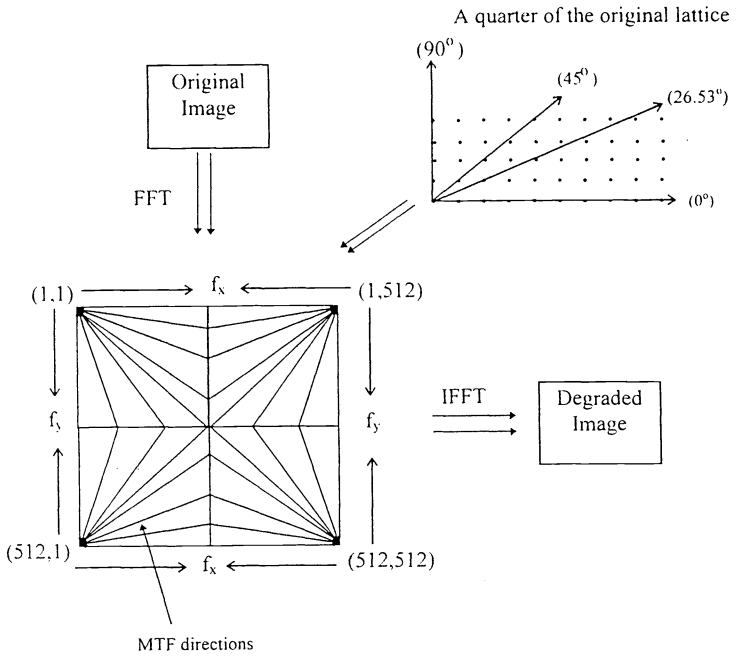

Fig. 7 Description of the degradation process.

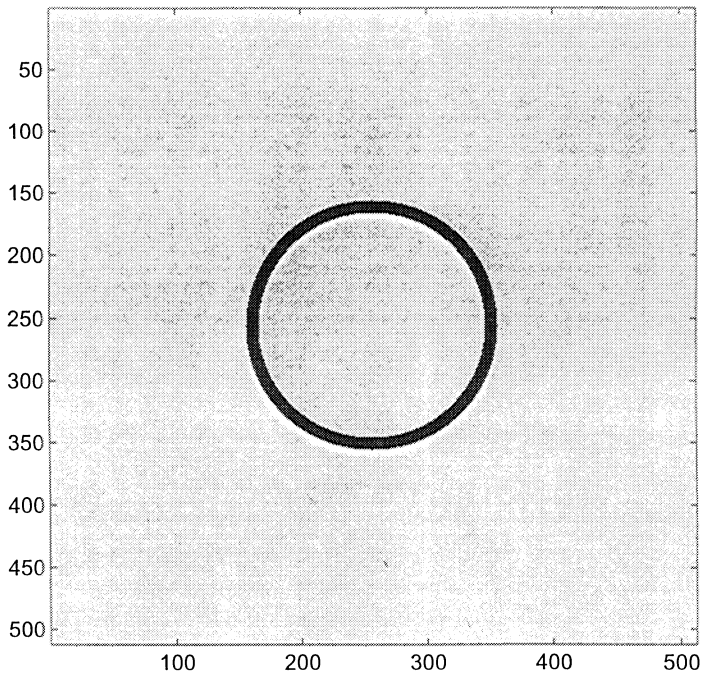

Fig. 8. Original Image.

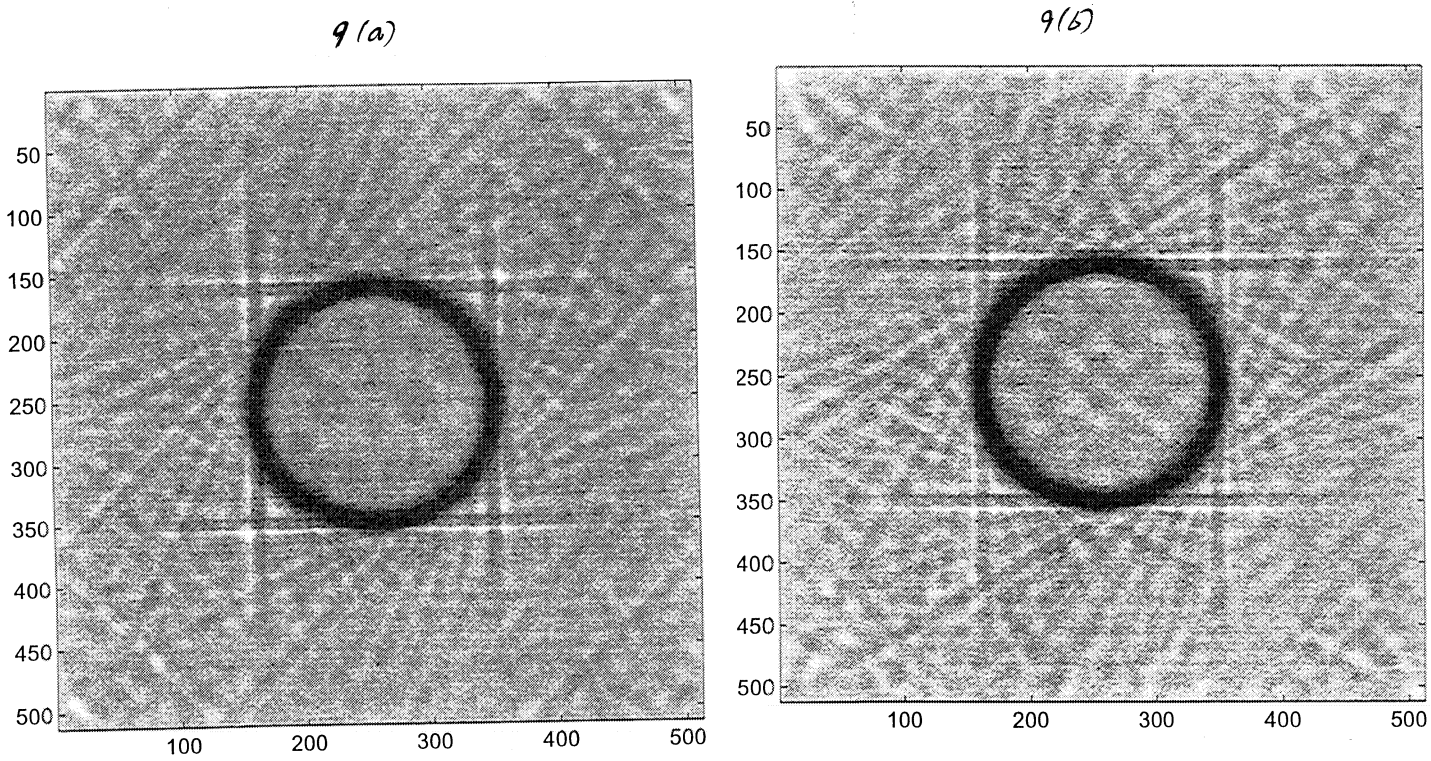

Fig. 9. Degraded image by a sampling MTF of 100 by 100 points lattice size , (a) Rectangular lattice (b) Hexagonal lattice.